LBL-25508
Preprint

Center for Advanced Materials

CAM

Submitted to Surface Science

Forward Focusing of Auger and Kikuchi Electrons for Surface Structure Determination: Ni(100) and Oxidized Mg(0001)

RECEIVED
LAWRENCE
BERKELEY LABORATORY

AUG 31 1988

LIBRARY AND
DOCUMENTS SECTION

H. Cronacher, K. Heinz, K. Müller, M.-L. Xu,
and M.A. Van Hove

June 1988

TWO-WEEK LOAN COPY

This is a Library Circulating Copy
which may be borrowed for two weeks.

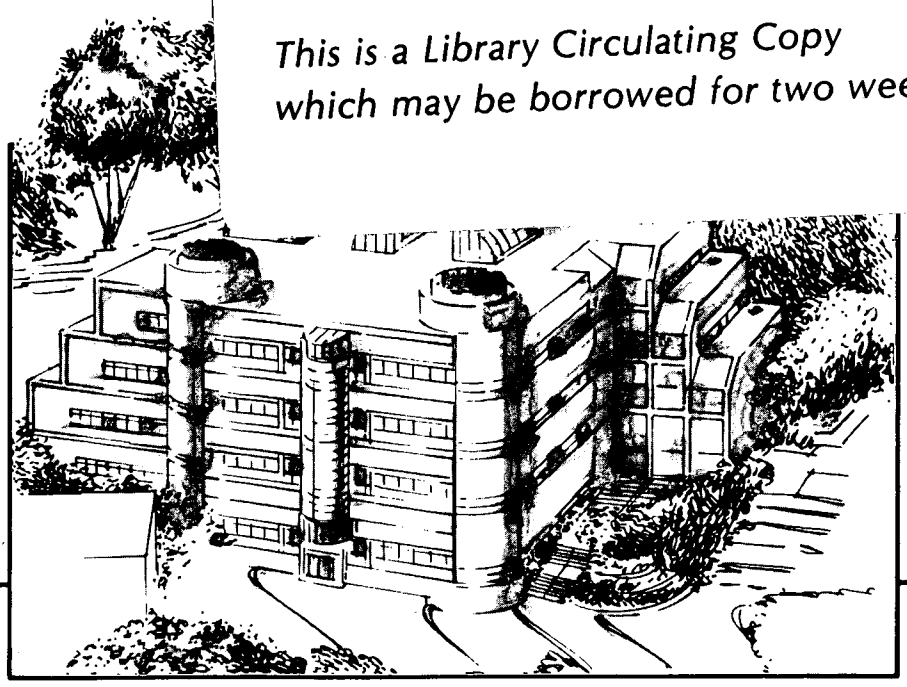

Materials and Chemical Sciences Division

Lawrence Berkeley Laboratory • University of California

ONE CYCLOTRON ROAD, BERKELEY, CA 94720 • (415) 486-4755

Prepared for the U.S. Department of Energy under Contract DE-AC03-76SF00098

LBL-25508 c.2

DISCLAIMER

This document was prepared as an account of work sponsored by the United States Government. While this document is believed to contain correct information, neither the United States Government nor any agency thereof, nor the Regents of the University of California, nor any of their employees, makes any warranty, express or implied, or assumes any legal responsibility for the accuracy, completeness, or usefulness of any information, apparatus, product, or process disclosed, or represents that its use would not infringe privately owned rights. Reference herein to any specific commercial product, process, or service by its trade name, trademark, manufacturer, or otherwise, does not necessarily constitute or imply its endorsement, recommendation, or favoring by the United States Government or any agency thereof, or the Regents of the University of California. The views and opinions of authors expressed herein do not necessarily state or reflect those of the United States Government or any agency thereof or the Regents of the University of California.

LBL-25508

Forward Focusing of Auger and Kikuchi Electrons for Surface Structure Determination: Ni(100) and Oxidized Mg(0001)

H. Cronacher, K. Heinz, K. Müller,
Lehrstuhl für Festkörperphysik,
Universität Erlangen–Nürnberg,
Erwin–Rommel–Strasse 1,
D–8520 Erlangen, FRG,
and
M.–L. Xu, M.A. Van Hove
Center for Advanced Materials,
Materials and Chemical Sciences Division
Lawrence Berkeley Laboratory
Berkeley, California 94720

June 28, 1988

Abstract

Angular profiles of "Kikuchi" and Auger electrons were measured and interpreted for a clean Ni(100) surface and a slightly oxidized Mg(0001) surface. Theoretical analysis of the data using forward focusing of the medium–energy electrons (500-1500 eV) shows that both Kikuchi and Auger electrons can be well represented as s-waves emitted from atomic sites. The Auger electron data are used to analyze the structure of slightly oxidized Mg(0001), yielding oxygen atom positions in the octahedral interstitial sites in the first two interlayer spacings of the metal.

1 Introduction

Structure determination with the help of forward-focused medium-energy electrons has recently been shown to have great potential [1],[2],[3],[4],[5],[6],[7],[8]. Suitable electrons have mostly been generated through photoemission and Auger emission, with kinetic energies in the range of 500 to 1500eV. In this paper, we start by investigating the same phenomenon with a different source of electrons: inelastically scattered electrons of similar energies, which can be called Kikuchi electrons to reflect the importance of scattering subsequent to their energy loss [9]. Several other authors [10],[11],[12],[13] have also investigated Kikuchi electrons. Gomoyunova et al[10] correctly interpreted angular Kikuchi electron distributions for Mo(100) in terms of peaks due to electrons emitted preferentially along atomic chains, but could not obtain a quantitative interpretation of their data.

Electrons with medium energies are strongly forward focused by atoms in their path, especially by atoms near the electron source. By that mechanism, peaks in angle-resolved electron distributions are produced that correspond to interatomic directions. These peaks can then be used to determine the geometrical surface structure by comparison with a corresponding theory. In the case of Ni(100), we apply a theory that assumes an s-wave initial state centered on nuclei and incor-

porates multiple scattering. We show that this theory provides an equally good description of Kikuchi and Auger electron angular distributions. This strengthens the same conclusion drawn earlier from the experimental observations [9].

In a second part, we analyze the structure of oxygen deposited on Mg(0001), with the help of Auger electrons generated in the oxygen atoms. It is shown that the forward focusing technique helps greatly in determining the oxygen site. The technique is particularly convenient for distinguishing between such sites as adsorption in an overlayer, and interstitial or substitutional absorption within the surface. Thus the oxidation state of a metal or other surface can be readily investigated for structure. Similar studies based on single scattering of photoelectrons have been performed on the NiO(100) surface. [14]

Previously[15], the O/Mg(0001) data used here have been analyzed with a plane-wave single-scattering model. This already provided a preliminary surface structure. The present work extends this analysis with a curved-wave single-scattering theory and with a complete multiple-scattering formalism.

Our multiple-scattering theory uses the formalism called "near-field expansion in clusters", described elsewhere[16]. It is specifically designed to describe forward focusing accurately and efficiently, despite the relatively high electron energies. Thereby the measured angular electron distributions can be modeled for many plausible surface structures [8].

2 Experiment

2.1 Data for O/Mg (0001)

The measurements for O/Mg (0001) were performed in a stainless steel UHV vessel with a base pressure of 10^{-10} mbar. Besides facilities for sample preparation such as an argon ion gun and indirect heating, the apparatus is provided with a conventional LEED optics, a separate Auger electron gun and spherical electron energy analyzer combined with a channeltron detector. As displayed in Fig.1 the sample can be rotated to face either the LEED optics or the Auger gun and analyzer. Optics and

analyzer are mounted on a turntable which is rotatable around the sample. In such a way angular profiles can be taken with sample position and incident beam direction fixed in space. Careful adjustment is necessary to ensure that during rotation the spectrometer remains focused on the primary beam's spot at the sample.

For the measurements presented here the analyzer is operated without preretardation, providing a resolution independent of energy. The distance between sample and spectrometer entrance slit is 23 mm, which determines the angular aperture to be 3 degrees (polar direction). The primary beam (5 μA, 2 keV) is made to hit the surface at 65° off normal with a diameter of almost 1 mm. The spectrometer energy is modulated with an amplitude of 2 eV and the corresponding ac signal of the channeltron is read by a lock- in amplifier. A personal computer stores the differentiated Auger spectra at each polar angle, which is varied in steps of 2° .

The Mg sample is a single crystal of 4N purity. Mechanical (1 μm grain) polishing was followed by electropolishing according to procedures known from the literature [17],[18], [19]. Several cycles of argon ion bombardment (500 eV, 15 min) and subsequent heating (500 K, 2 h) led to an almost clean surface with faint impurities of carbon and oxygen as displayed in Fig. 2a. The LEED pattern of this almost clean surface is given in Fig. 3a showing relatively sharp diffraction spots and low background.

With the surface exposed to oxygen at room temperature the oxygen signal at 503 eV starts growing while the Mg signal at 45 eV simultaneously decreases. The ratio of peak-to-peak heights of both signals can be taken as a measure for the coverage or degree of oxidation. So, for Mg/O $\geq$ 20 the surface can be viewed as practically clean with Auger spectra and LEED patterns as displayed in Fig. 2a and Fig. 3a, respectively. For Mg/O $<$ 20 the low energy part of the Auger spectrum changes significantly as demonstrated by Fig. 2b. A new peak appears at 27 eV which can be interpreted by a cross transition $Mg^{2+}(L_{2,3})$ $O^{2-}(L_1)$ Mg(V) growing in amplitude with increasing oxygen exposure. The same holds for the 34 eV peak, which for the clean surface is a $Mg(L_1\ L_{2,3}\ V)$ transition but with increasing oxygen density the signal is dominated by the cross transition $Mg^{2+}(L_{2,3})$

$O^{2-}(L_{2,3})$ $O^{2-}(L_{2,3})$. The appearance of cross transitions demonstrates that oxygen is chemisorbed rather than physisorbed. Figs. 3b-d display the LEED patterns as developing with decreasing ratio Mg/O. For Mg/O < 10 the spots start to broaden with simultaneous appearance of background intensity. For Mg/O $< 1/20$ (not shown) the background dominates the pattern, i.e. spots show only very weak intensities. This demonstrates that with increasing oxidation long range order disappears within the surface slab. Similar observations were reported earlier[18],[19], [20] together with intermediate or final development of superstructure spots which, however, are not observed in the present investigation.

Angular resolved Auger measurements were taken for different stages of oxidation and for the transitions Mg (34 eV), MgO (34 eV) and O (503 eV). In the present work we concentrate on the oxygen transition at 503 eV. Polar profiles were measured for azimuths both along [210] and [100] directions as displayed in Fig. 4 for different ratios of Mg/O. The data correspond to the peak-to-peak heights H_{pp} of the transitions. The vertical error bar is given at the right end of the profiles, the angular uncertainty is $\pm$ 0.2 degrees. Although the vertical error bar is larger than some of the peaks, most of the latter could be safely reproduced by different measurements. The observed asymmetry in Fig. 4 could be due to oxygen favoring one type of double-height steps or due to the unbalancing of terraces by adsorption [equal probability of the two possible surface terminations of hcp(0001) would produce symmetrical curves, as was observed for clean Mg(0001) using Mg transitions]. As demonstrated by Fig. 4, the profiles do not dramatically change with decreasing ratio Mg/O. So, only the profiles for Mg/O $= 6$ are subject to a theory - experiment fit presented in section 5.

2.2 Data for clean Ni(100)

The measurements for angular dependent Auger emission from Ni(100) were performed in a much different way. As described in detail earlier[9], a conventional 3-grid LEED optics was used to detect inelastic electron intensities by a spot photometer. In this way both Kikuchi intensities and - by modulating the suppressor

voltage - Auger intensities were accessible at any point of the screen. Polar and azimuthal profiles were taken for the Kikuchi pattern at 850 eV and for the Auger L_3VV transition at the same energy. The angular resolution for polar profiles varies between 4.9° and 5.3°, while for azimuthal profiles rather large values result, i.e. 9.6° for $\theta = 29°$ and 15° for $\theta = 18°$.

3 Theory

A recent theoretical formalism has been developed to describe both the pronounced forward–focusing and the multiple scattering that prevail at the medium electron energies (200—5000 eV). Forward focusing is due to the individual atomic scattering amplitude: a plane wave representing an electron scatters primarily within a forward cone which has a half-width of about 10°. This requires inclusion of high angular momenta, e.g. up to $l_{max} = 19$ for Ni at 1000 eV.

Multiple scattering is important when electrons scatter from successive atoms along a chain of atoms. This is very common in crystalline materials, including clean and modified surfaces. The combination of high angular momenta in atomic scattering and multiple scattering, as well as high energies, prevents the use of standard LEED formalisms. Therefore, the method called "near–field expansion in clusters" (NFEC) was developed, which is based on the "Taylor series, magnetic quantum number expansion" (TS-MQNE), first used to describe angle-resolved photoelectron emission fine structure (ARPEFS) [21,22]. The NFEC method is described in reference[16] while its application to forward focusing of Auger electrons is explored in references[7],[8].

Two levels of single-scattering approximation were applied in our simulations of Auger emission from O/Mg(0001). A number of structures was first analyzed with a plane-wave version of single-scattering theory [15]. Another set of structures, partly overlapping with the first set, was analyzed with a more accurate curved-wave single-scattering theory: this is the NFEC theory limited to one scattering only.

The assumption of an s–wave emission can be supported by the theory of Auger emission [23]. If we assume a spherically symmetric potential as probably valid for the deeper levels, selection rules give for the final–state angular momentum l_f:

$$|l_l - |l_j - l_k|| \leq l_f \leq l_j + l_k + l_l$$

and

$$l_j + l_f + l_k + l_l = \text{even},$$

if l_j, l_k, l_l are the three levels involved the transition.

Let us apply these relations to the case of the $KL_{2,3}L_{2,3}$ transition in oxygen, which involves the angular momenta $(l_j, l_k, l_l) = (0, 1, 1)$. They imply that $0 \leq l_f \leq 2$ and $l_f + 2 =$ even, i.e. $l_f = 0$ and/or 2. At our higher energies, the $l_f = 2$ contribution is relatively small.

For the theoretical analysis, we used 20 phase shifts which are based on the Moruzzi-Janak-Williams potential [24] for Ni, and on a Tong-Puga surface potential [25] built from Herman-Skillman wave functions for O and Mg. The lattice parameters are a=3.52 Å for Ni and a=3.21 Å, c=5.21 Å for Mg. Debye temperatures for Ni, Mg, O are 335K, 400K and 843K respectively. An energy-dependent electron mean free path was used, with values of 22.5 Å at 850 eV and 17.0 Å at 503 eV. Note that the incident primary electrons are damped as they penetrate into the surface, such that the probability of electrons leaving any given layer decays exponentially with depth. This damping is also simulated with mean free paths. An acceptance angle of 5.0° in polar angle and azimuth was used in the computation to represent the experimental aperture.

4 Application to Ni(100)

Figures 5 and 6 show measured and calculated electron distributions from Ni(100). Measured Kikuchi and Auger electron distributions are included separately. It is readily seen that these two kinds of electrons produce very similar distributions. The differences are of the size of the experimental uncertainties (see the deviations from the expected four-fold and mirror-plane symmetries in the $\theta = 29°$ azimuthal

plot of Figure 6).

The electron distributions of Figures 5 and 6 were calculated with the same settings for energy and angle as in the experiment. These calculated distributions fit the large majority of experimental peaks well. The main exceptions occur at the larger angles in the polar plot for $\phi = 30°$. These correspond to weak intensities, where we have previously seen that the multiple- scattering formalism and Auger-based experiments do not match well peak for peak [8]. This may be a limitation of the s-wave assumption.

Only the peaks in the $\phi = 0°$ polar plot and the normal-emission peak in the $\phi = 30°$ polar plot are forward- focusing peaks.

All other peaks are interference peaks due to combinations of paths that interfere to produce maxima in the distributions. This illustrates the great danger of assuming that peaks must necessarily correspond to interatomic axes. One is not likely to make that mistake with a simple fcc(100) surface, but with complex structures it is not a priori possible to tell which peaks are due to forward focusing and which are due to interference. Thus a model calculation is required to understand the measured distributions in those circumstances. This will be quite obvious in the case of O/Mg(0001), described in the next section.

5 Structure of O/Mg(0001)

As described in section 2, we have strong evidence that oxygen can penetrate into the Mg(0001) surface under our experimental conditions. Therefore, we have simulated angle-resolved Auger emission distributions for a variety of oxygen positions, both above the Mg surface and below it.

The models which we have tested with curved-wave single scattering assume a single oxygen atom surrounded by an infinite clean Mg(0001) surface. The other calculations, based on the more exact curved-wave formalism, have 1/6 coverage of oxygen, arranged arbitrarily and for computational convenience in a (2x3) monolayer lattice in a finite cluster. The coverage of oxygen is close to being irrelevant

in the theory, because the chance of electrons emitted from one oxygen atom being significantly perturbed by other oxygen atoms is very small at our low coverage.

The models are illustrated in Figure 7 and listed next, using the ABAB... registry notation to denote Mg layer stackings, with lower case letters applying to oxygen and parentheses denoting substitution for Mg atoms:

- (a)BABA... , A(b)ABAB... and AB(a)BABA... : substitutional absorption in the place of Mg atoms; included is a model in which the substituted Mg atom of the top Mg layer moves into an overlayer position at an hcp lattice site next to the oxygen;

- cABAB... and bABAB... : overlayer adsorption in fcc or hcp hollow sites;

- cAcBABA... : simultaneous adsorption in fcc hollow sites and interstitial octahedral absorption between the first and second Mg layers;

- AcBABA... , ABcABAB... and AcBcABAB... : underlayer interstitial absorption in octahedral sites between the first and second Mg layers, or between the second and third Mg layers, or between both sets of layers;

- AaBABA... and AbBABA... : underlayer interstitial absorption in tetrahedral sites between the first and second Mg layers;

- AcBcAcBABA... : interstitial octahedral absorption below the first three Mg layers.

Simultaneous adsorption in different sites is modeled with incoherent superposition of the distributions due to each separate site. We have tested these basic models against each other by use of the two levels of single-scattering approximation described in section 3. With the plane-wave single-scattering calculations, many models could already be excluded.

The quality of the curved-wave single-scattering approximation for this case is illustrated in Figure 8 (curves e vs. f) by comparison with multiple-scattering results: it is more than adequate for our structural determination. The reason why this single-scattering approximation is so good in this case is that the interstitial oxygen positions are not aligned with chains of Mg nuclei. Thus there is relatively little multiple scattering taking place along chains of atoms, which would cause such

effects as defocusing described in reference[7].

After a large number of variations of interlayer spacings within the above models, the best among them appears to be the one labeled AcBcABAB..., i.e. interstitial absorption below the first two Mg layers, with interlayer spacings of 1.35Å between Mg and O layers and the bulk value of 2.605Å. Representative Auger electron distributions are shown in Figure 8, using the curved-wave single-scattering approximation. The best structure is confirmed by a multiple-scattering test performed on this structure and shown in Figure 8.

Remaining discrepancies between the theoretical and experimental curves could be due to various factors. Besides experimental inaccuracies, uncertainties may be introduced by our s–wave assumption and by not allowing for the possibility of other adsorption or absorption sites, together with local oxygen-induced distortions.

Thus the best structure model for 1/6 coverage of oxygen on Mg(0001) is found to have octahedrally-bonded interstitial oxygen within the first two magnesium interlayer spacings, which are thereby expanded by about 0.1Å from 2.605Å to 2.70Å .

Since the oxygen coverage is not a sensitive quantity in our analysis, our forward-focusing results do not imply a confirmation of the experimental 1/6 monolayer determination. Also, we have not attempted to determine the relative concentration of oxygen at different depths. Clearly, this could be done in principle by optimizing the incoherent mix of contributions from different depths. But the level of agreement between experiment and theory is not good enough to embark on such an analysis.

6 Conclusions and Discussion

6.1 Kikuchi Electron Emission

With the help of multiple-scattering calculations, we have explored the close similarity between experimental angular distributions of Kikuchi and Auger electrons emitted from Ni(100). It is found that an isotropic s-wave centered on an atomic nucleus describes well the initial wave after the energy loss process. The same s-wave

model can therefore be used for both Kikuchi and Auger electrons.

It is pointed out that not only forward-focusing peaks appear in such experiments: interference peaks can be just as prominent. As was already discussed previously [7], there does not seem to be an easy way to distinguish these types of peaks, except by making computer simulations. Therefore, especially with complicated surface structures, it is necessary to simulate the emission process to obtain reliable structural information with this technique.

6.2 Structure of Oxidized Mg(0001)

With angle-resolved Auger electron emission from oxygen, we have determined the surface structure of slightly oxidized Mg(0001). We find the oxygen atoms to occupy octahedral sites below the first and second Mg layers, causing a small expansion by about 0.1$\AA$ of the corresponding interlayer spacings.

The absolute coverage would be difficult to determine by this method. The relative concentration of oxygen at different depths could possibly be obtained, if the agreement between experiment and theory were better.

The technique of forward focusing of electrons (whether Auger, Kikuchi or photoemitted electrons) has once again proven itself very capable of an otherwise more difficult task: the determination of the adsorption or absorption site of adatoms at surfaces.

An important observation is made here for the case when the emitting atoms are not in positions aligned with chains of nearby atoms. Then the single-scattering approximation is very good and quite sufficient for structural determination. The reason is that few nearby atoms are then shielded from the emitter by other atoms, so that multiple scattering from one atom to another is unlikely. The basic assumption here is that the forward-scattering cone of any nearby atom is sufficiently narrow to not include other nearby atoms.

Acknowledgements

We thank J.J. Barton for most helpful discussions. The theoretical part of this work was supported by the Army Research Office. Institutional support came from the Director, Office of Energy Research, Office of Basic Energy Sciences, Materials Sciences Division of the U.S. Department of Energy under Contract No. DE-AC03-76SF00098.

References

[1] W.F. Egelhoff Jr. *Phys. Rev. B* **30** (1984) 1052.

[2] W.F. Egelhoff Jr. *Phys. Rev. Lett.* **59** (1987) 559.

[3] S.A. Chambers, S.B. Anderson, and J.H. Weaver. *Phys. Rev. B* **32** (1985) 581.

[4] S.A. Chambers, S.B. Anderson, and J.H. Weaver. *Phys. Rev. B* **32** (1985) 4872.

[5] S.A. Chambers, H.W. Chen, I.M. Vitomirov, S.B. Anderson, and J.H. Weaver. *Phys. Rev. B* **33** (1986) 8810.

[6] S.A. Chambers, S.B. Anderson, H.W. Chen, and J.H. Weaver. *Phys. Rev. B* **35** (1987) 2592.

[7] M.L. Xu, J.J. Barton, and M.A. Van Hove. Phys. Rev. B (to be published).

[8] M.L. Xu and M.A. Van Hove. Surf. Sci.(to be published).

[9] H. Hilferink, E. Lang, and K. Heinz. *Surf. Sci.* **93** (1980) 398.

[10] M.V. Gomoyunova, I.I. Pronin, and I.A. Shmulevitch. *Surf. Sci.* **139** (1984) 443.

[11] A. Mosser, S. Shindo, and Y. Adachi. *Phys. Status Solidi (a)* **43** (1977) 295.

[12] R.M. Stern and H. Taub. *Phys. Rev. Lett.* **20** (1968) 1340.

[13] J.L. Robins, R.L. Gerlach, and T.N. Rhodin. *J. Appl. Phys. Letters* **8** (1966) 12.

[14] M. Sagurton, E.L. Bullock, R. Saiki, A. Kaduwela, C.R. Brundle, and C.S. Fadley. *Phys. Rev. B* **33** (1986) 2207.

[15] H. Cronacher. 1985. Diploma (unpublished).

[16] J.J. Barton, M.L. Xu, and M.A. Van Hove. Phys. Rev. B (in press).

[17] W. Tegart. *Electrolytic and Chemical Polishing of Metals in Research and Industry.* Pergamon Press, New York, 1959.

[18] B.E. Hayden, E. Schweizer, R. Koetz, and A.M. Bradshaw. *Surf. Sci.* **111** (1981) 26.

[19] H. Namba, J. Darville, and J.M. Gilles. *Surf. Sci.* **108** (1981) 446.

[20] S.A. Flodstrom and C.W.B. Martinsson. *Surf. Sci.* **118** (1982) 513.

[21] J.J. Barton and D.A. Shirley. *Phys. Rev. B* **32** (1985) 1892.

[22] J.J. Barton and D.A. Shirley. *Phys. Rev. B* **32** (1985) 1906.

[23] R.G. Weissmann and K.Muller. *Surf. Sci. Rep.* **1** (1981) 251.

[24] V.L. Moruzzi, J.F. Janak, and A.R. Williams. *Calculated Electronic Properties of Metals.* Pergamon, New York, 1978.

[25] S.Y. Tong. private communication.

Figure Captions

Figure 1. Part of the central experimental setup. The broken line indicates the limits of rotation for the spectrometer.

Figure 2. Auger spectra for the almost clean surface (a) and in the low energy region for decreasing values of Mg/O (b).

Figure 3. LEED patterns for (a) Mg/O > 20, E = 103 eV, (b) Mg/O = 6, E = 105 eV, (c) Mg/O = 4, E = 106 eV and (d) Mg/O = 1, E = 105 eV.

Figure 4. Polar profiles of the O-$KL_{2,3}L_{2,3}$ (503 eV) transitions along [100] and [210] azimuths for different ratios Mg/O.

Figure 5. Experimental angle-resolved distributions of emitted Kikuchi electrons (dashed lines) and Auger electrons (dash-dot lines) for Ni(100), compared with theoretical calculations (full lines). The kinetic energy is 850eV. The two panels show the polar-angle dependence for two fixed azimuths ϕ ; $\phi = 0°$ refers to the [011] crystallographic direction and $\theta = 0°$ corresponds to normal emission. The vertical scales have been arbitrarily normalized to allow comparison of peaks.

Figure 6. As Figure 5, but showing with polar plots the azimuthal dependence at two fixed polar emission angles θ ; $\phi = 0°$ corresponds to the [011] direction.

Figure 7. Adsorption and absorption sites on Mg(0001).

Figure 8. Calculated and measured polar-angle distributions of emitted O($K_{2,3}L_{2,3}$) Auger electrons (530 eV) from O/Mg(0001) in the [210] azimuth (right panels) and [100] azimuth (left panels). For the calculated curves, different adsorption

and absorption sites, as labeled in the text, are assumed: (a) cABABAB.... (b) AcBABAB.... (c) ABcABAB.... (d)cAcBABAB.... (e) AcBcABAB.... with the curved-wave single-scattering model and (f) AcBcABAB.... with multiple-scattering model. The dot-dash line (g) gives the experimental data, peaks being emphasized by vertical bars.

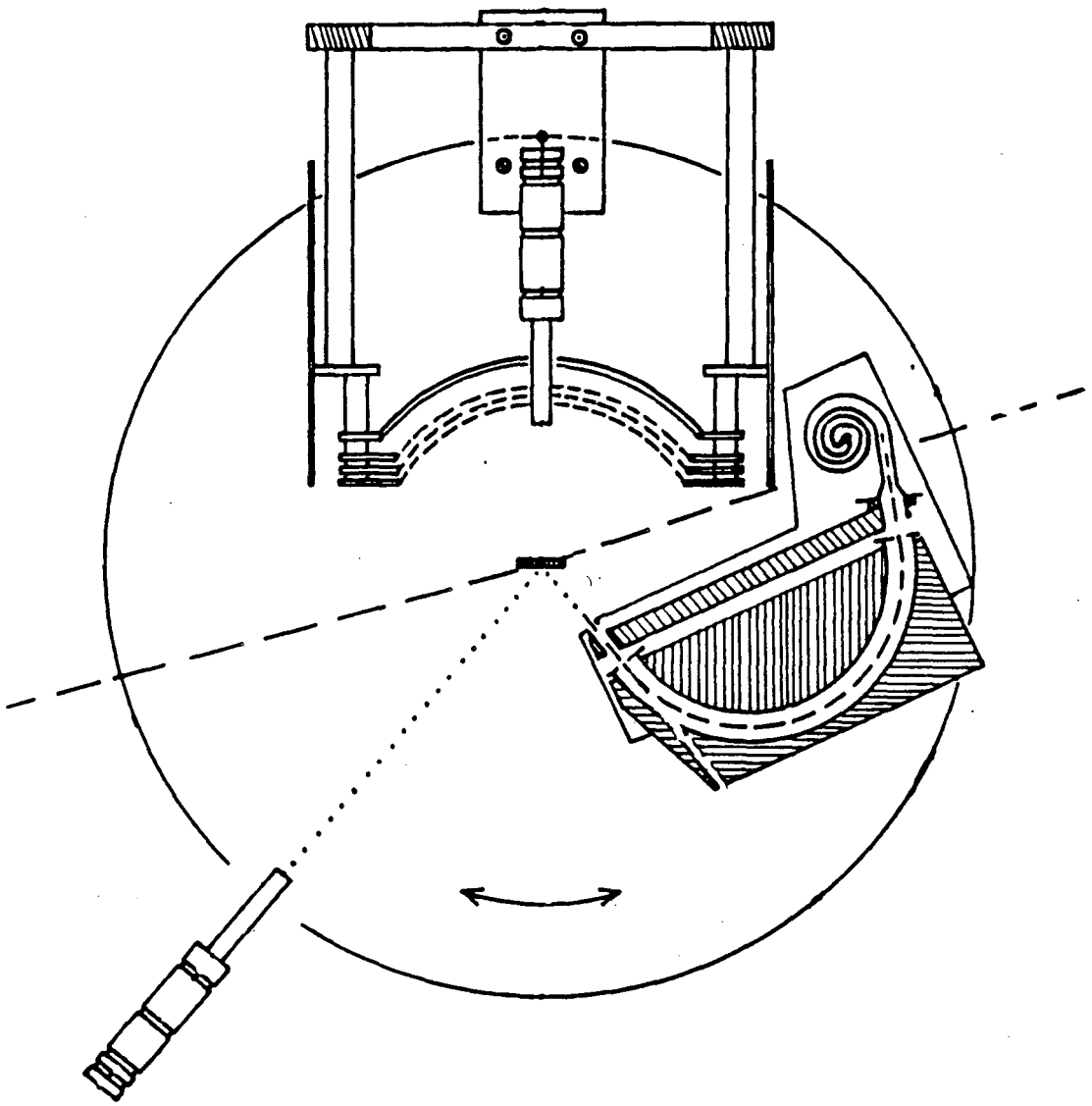

XBL 885-1862

Fig. 1

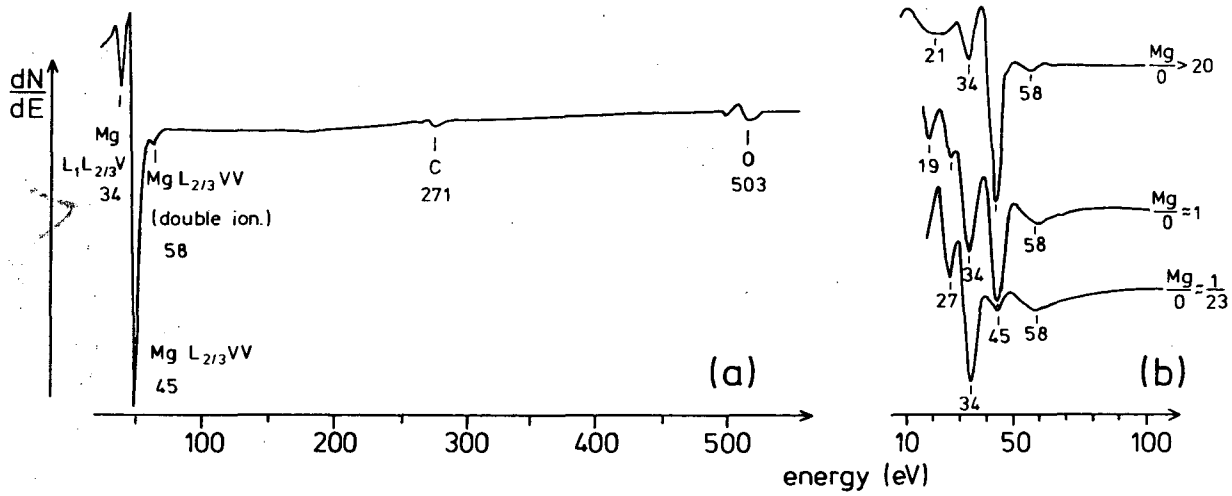

XBL 885-1863

Fig. 2

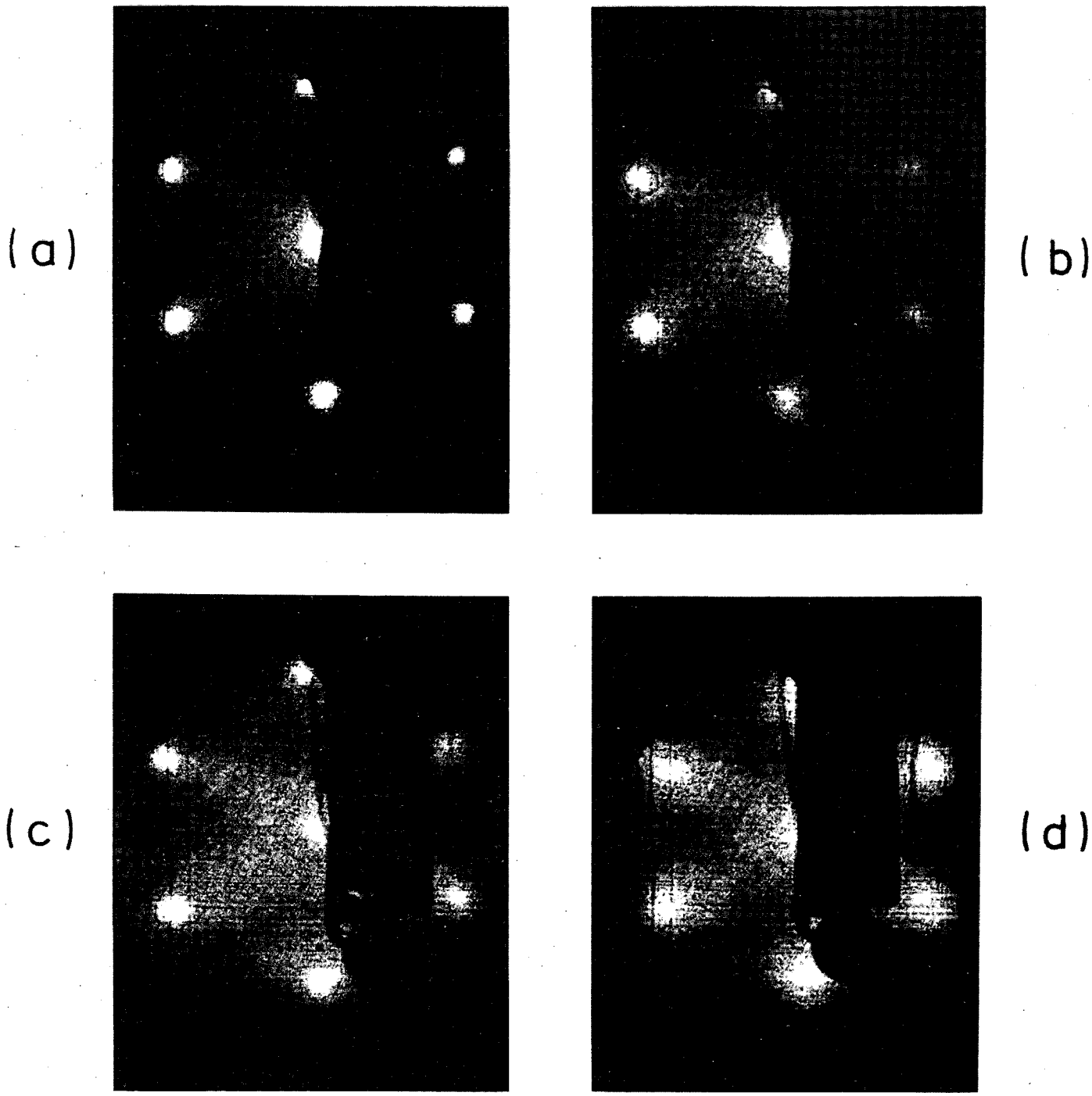

XBB 885-5275

Fig. 3

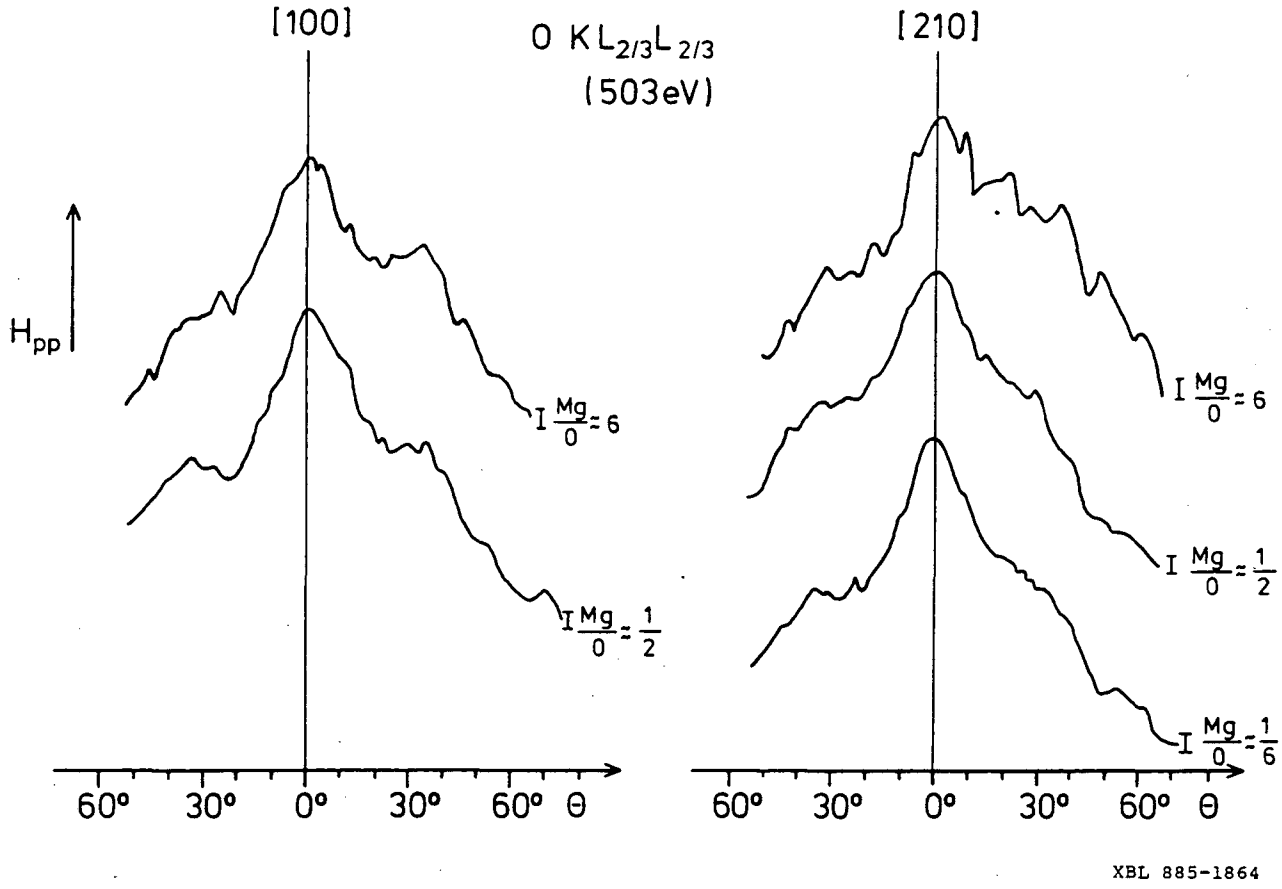
[100]
O $KL_{2/3}L_{2/3}$
(503eV)
[210]
H_{pp}
$I\frac{Mg}{O} \simeq 6$
$I\frac{Mg}{O} \simeq \frac{1}{2}$
$I\frac{Mg}{O} \simeq 6$
$I\frac{Mg}{O} \simeq \frac{1}{2}$
$I\frac{Mg}{O} \simeq \frac{1}{6}$
60° 30° 0° 30° 60° Θ
60° 30° 0° 30° 60° Θ
XBL 885-1864

Fig. 4

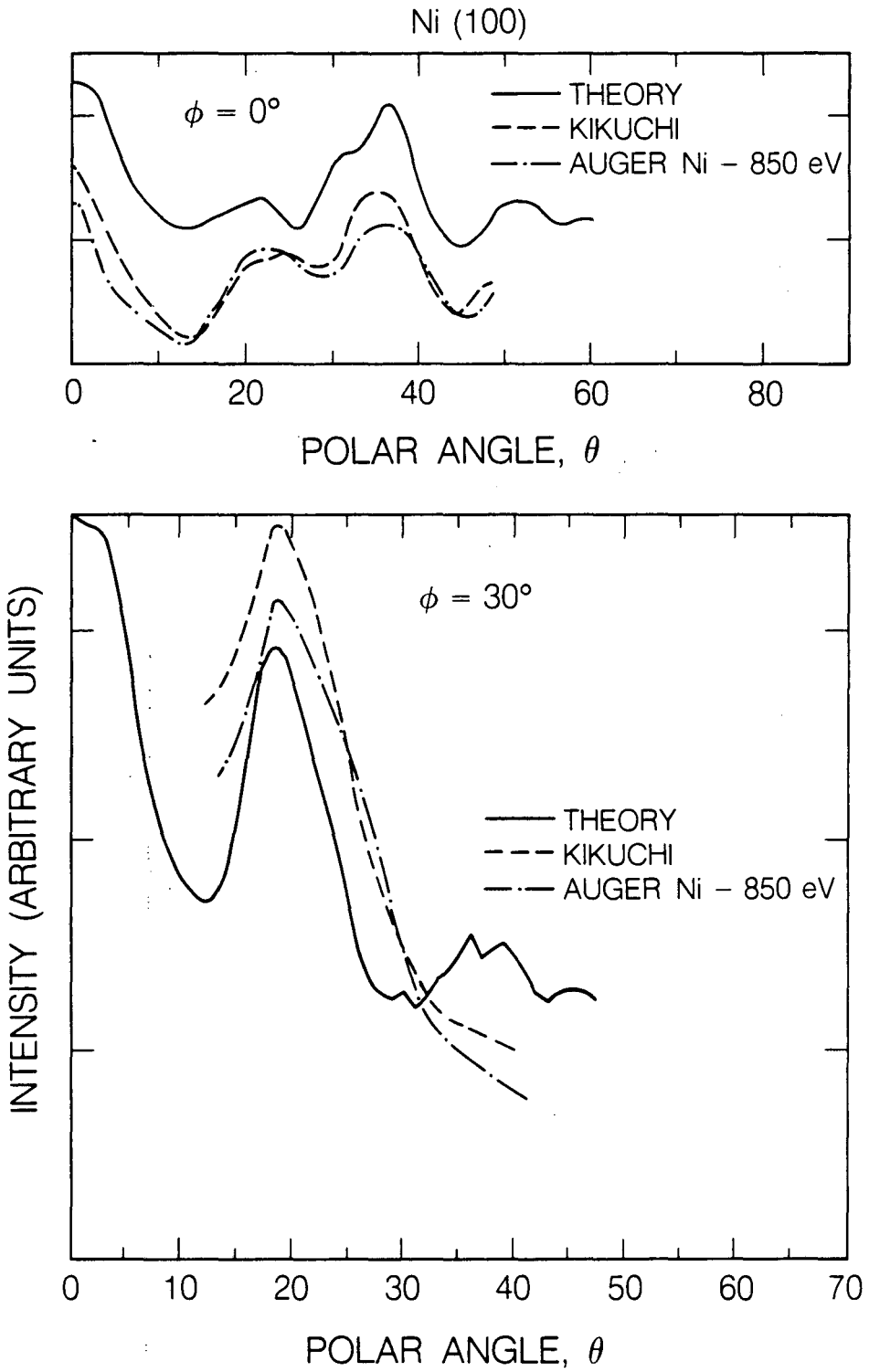

XBL 885-10232

Fig. 5

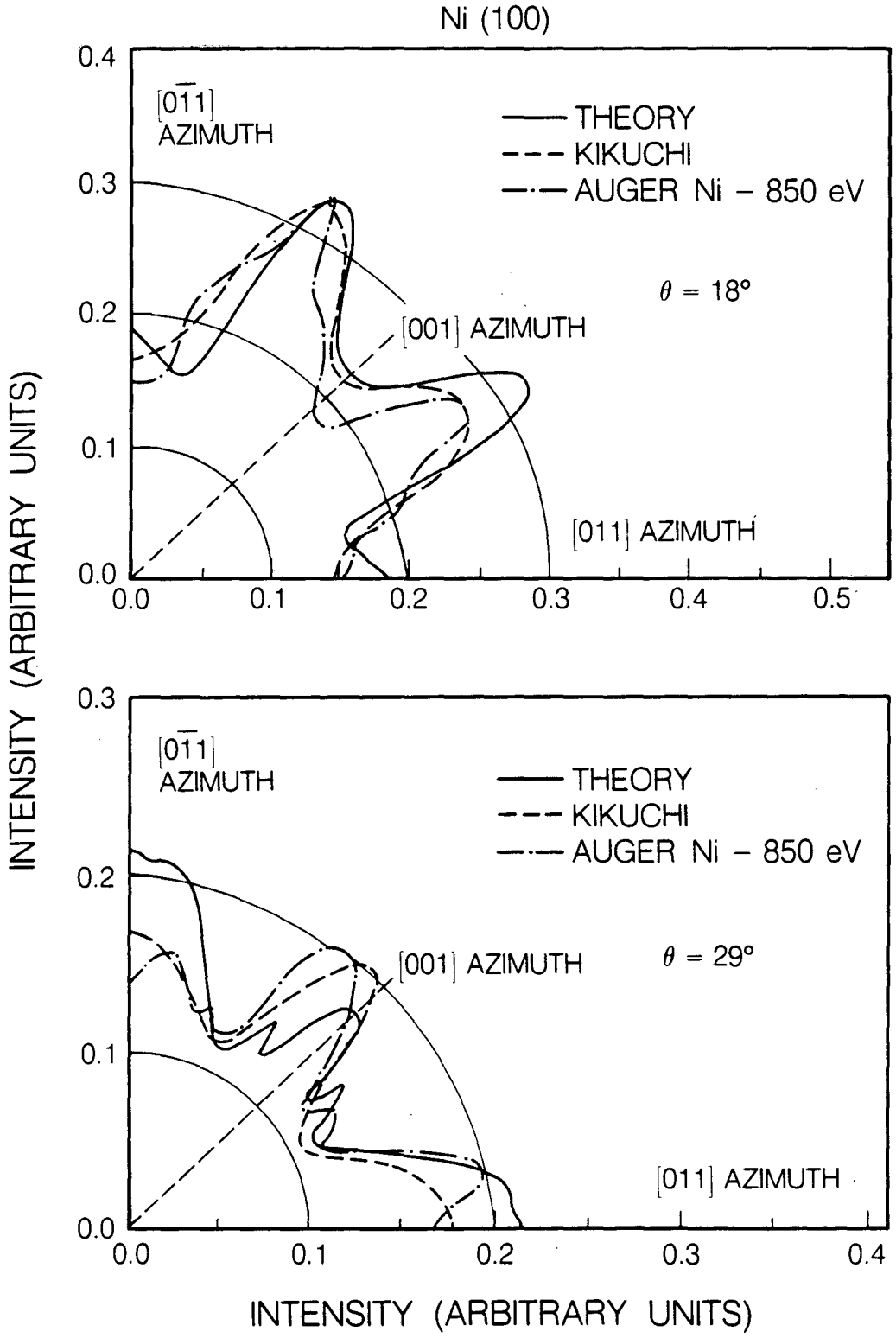

XBL 885-10229

Fig. 6

SITES ON Mg (0001)

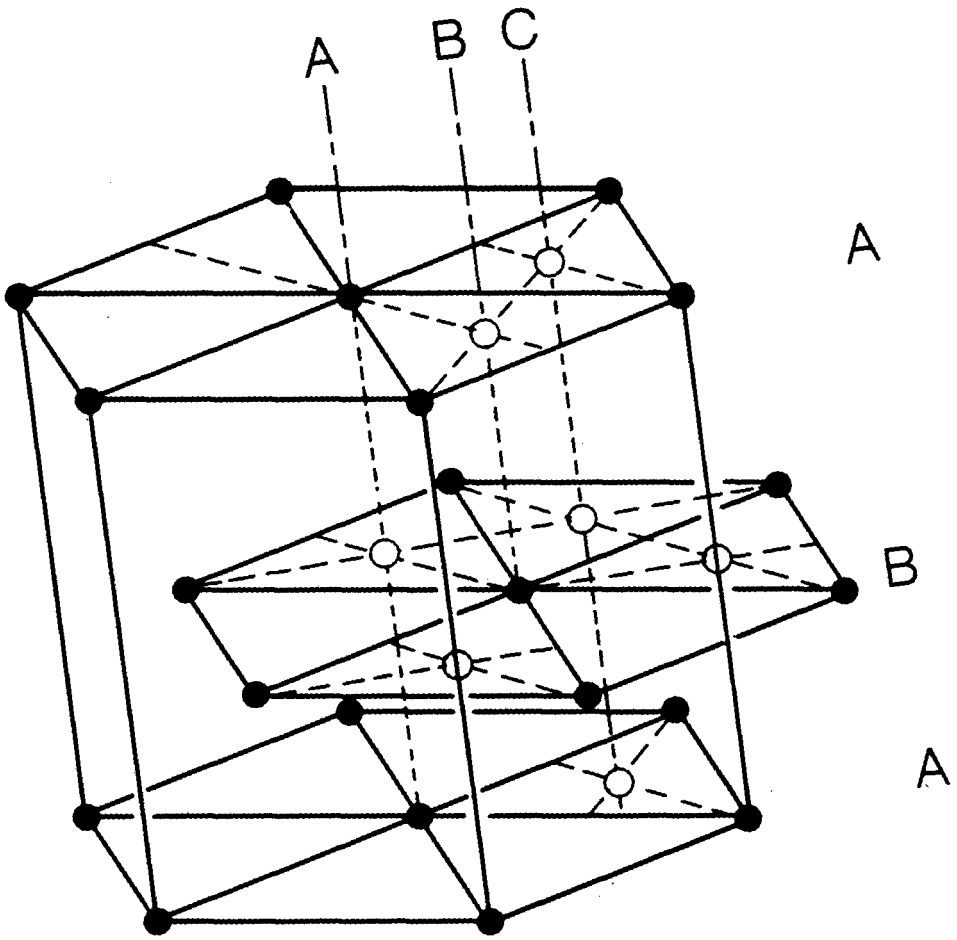

XBL 885-10228

Fig. 7

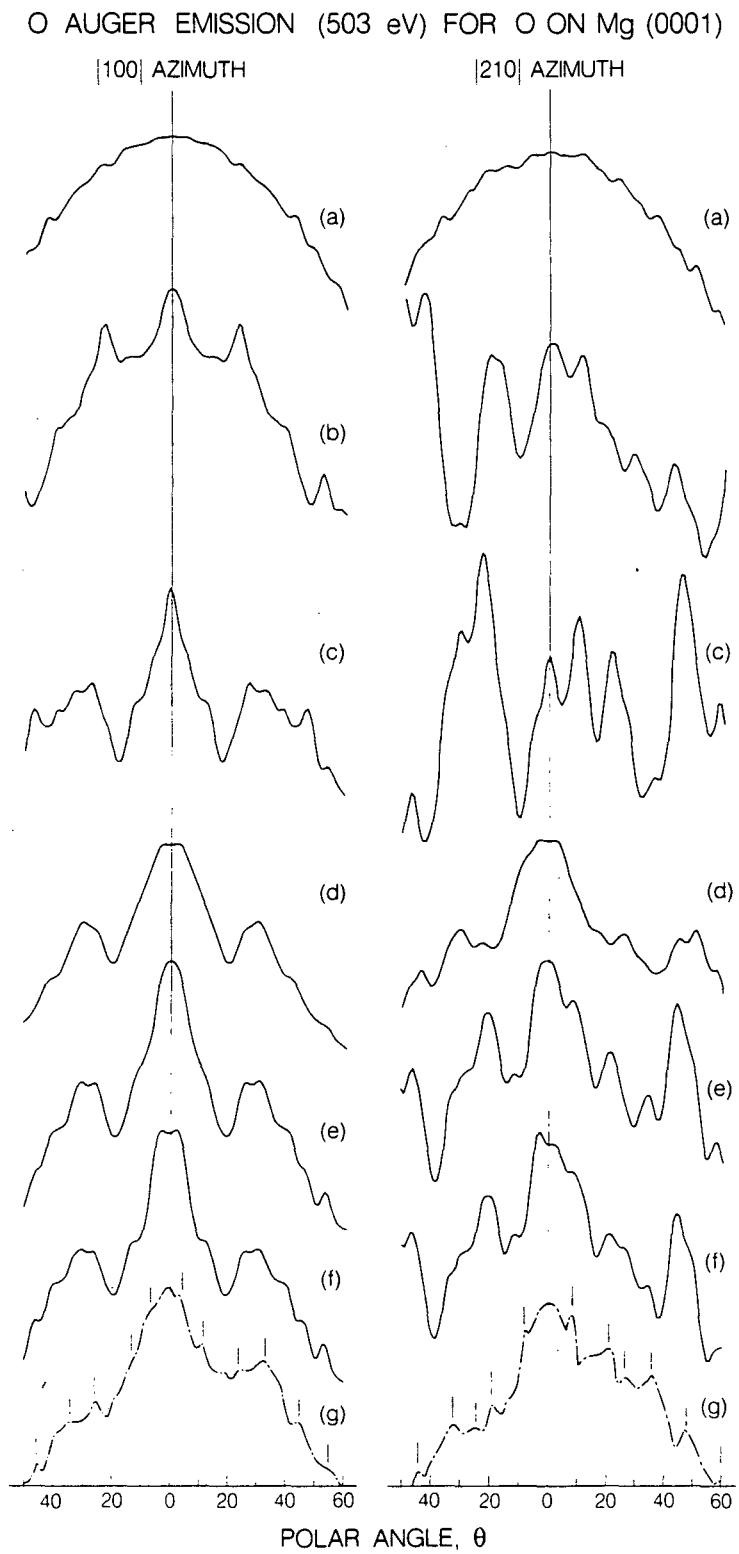
O AUGER EMISSION (503 eV) FOR O ON Mg (0001)
|100| AZIMUTH
|210| AZIMUTH
(a)
(b)
(c)
(d)
(e)
(f)
(g)
40 20 0 20 40 60
POLAR ANGLE, θ

Fig. 8

LAWRENCE BERKELEY LABORATORY
TECHNICAL INFORMATION DEPARTMENT
UNIVERSITY OF CALIFORNIA
BERKELEY, CALIFORNIA 94720